THE JOURNAL OF PHYSICAL CHEMISTRY C

Article

pubs.acs.org/JPCC

Terms of Use CC-BY

Determining the Exciton Diffusion Length in a Polyfluorene from Ultrafast Fluorescence Measurements of Polymer/Fullerene Blend Films

A. Bruno,[†] L. X. Reynolds,[†,§] C. Dyer-Smith,[†,‡,§] J. Nelson,*[,‡,§] and S. A. Haque*[,†]

[†]Department of Chemistry and Centre for Plastic Electronics, Imperial College London, South Kensington Campus, London SW7 2AZ, United Kingdom

[‡]Department of Physics and Centre for Plastic Electronics, Imperial College London, South Kensington Campus, London SW7 2AZ, United Kingdom

[§]Grantham Institute for Climate Change, Imperial College London, South Kensington Campus, London SW7 2AZ, United Kingdom

Supporting Information

ABSTRACT: Emission quenching is studied in systems composed of [9,9-dioctylfluorene-co-*N*-(4-butylphenyl)-diphenylamine] (TFB) and various concentrations of three different types of acceptors: [6,6]-phenyl-C61 butyric acid methyl ester (mono-PCBM) and its multiadduct analogues bis-PCBM and tris-PCBM. We find that the degree of emission quenching for a given fullerene concentration decreases as the PCBM adduct number increases, while the microstructure, as observed with transmission electron microscopy, becomes more coarse. These observations are rationalized in terms of possible differences in the miscibility of fullerenes in the polymer and different excitation dissociation rates. We also extract a value for the exciton diffusion length in TFB of 9.0 ± 2 nm from ultrafast fluorescence decay measurements. The results have been confirmed with independent measurements.

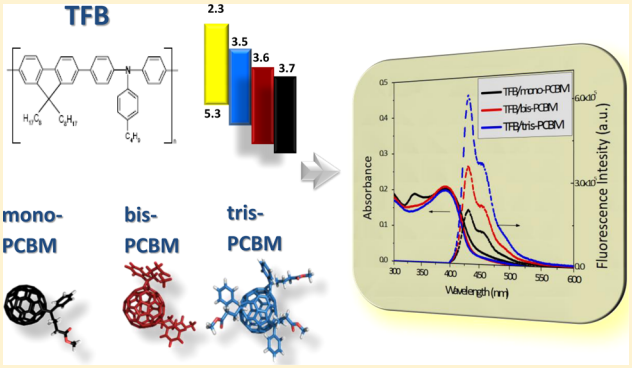

INTRODUCTION

Solution-processed organic photovoltaic (OPV) devices made from blend films of a conjugated polymer with a fullerene derivative are of great interest because of their potential for low cost manufacture and because they are flexible and lightweight. Although recent bulk heterojunction single-layer devices have reached certified efficiencies as high as 10%,[1,2] a more complete understanding is needed of how the chemical structure of the materials and physical microstructure of the polymer/fullerene blend film influence photophysical processes within the device. Photocurrent generation in a polymer/fullerene OPV device follows from the absorption of a photon in the polymer (donor), diffusion of the photogenerated exciton toward a fullerene (acceptor), dissociation of the exciton to generate a geminate charge pair, separation of the charge pair, and charge transport toward the contacts with an external circuit. Efficient dissociation of the exciton is thus a prerequisite for efficient photocurrent generation. In this scheme, exciton dissociation competes with the radiative and nonradiative decay of the exciton as well as with nondissociative energy transfer at the interface. The efficiency of dissociation depends on the exciton diffusion length in the polymer, L_{ex}, relative to the distance from the point of photon absorption (and thus exciton generation) to the interface with the acceptor material (referred to here as the domain size) as well as the energy difference, ΔE, between the singlet exciton and the geminate pair state. While intimate mixing of donor and acceptor phases would ensure efficient exciton dissociation, these conditions also encourage charge recombination. Therefore, a certain degree of phase segregation is advantageous for photocurrent generation, so long as it does not compromise the exciton dissociation efficiency.[3,4] In the ideal case, pure donor and acceptor domain sizes comparable to exciton diffusion lengths would be desirable for efficient charge photogeneration and device performance. Knowledge of the exciton diffusion length of the donor polymer is therefore essential for the optimization of film microstructure and nanomorphology; this in turn is necessary for efficient charge separation and device performance.[5−8]

Photophysical measurements of exciton dynamics such as photoluminescence (PL) are widely used in the characterization of new OPV material combinations, both to determine the conditions that lead to exciton dissociation in any given case[9] and, when used together with other measurements of charge generation, to determine the extent to which poor exciton

Received: May 21, 2013
Revised: August 12, 2013
Published: September 24, 2013

 © 2013 American Chemical Society

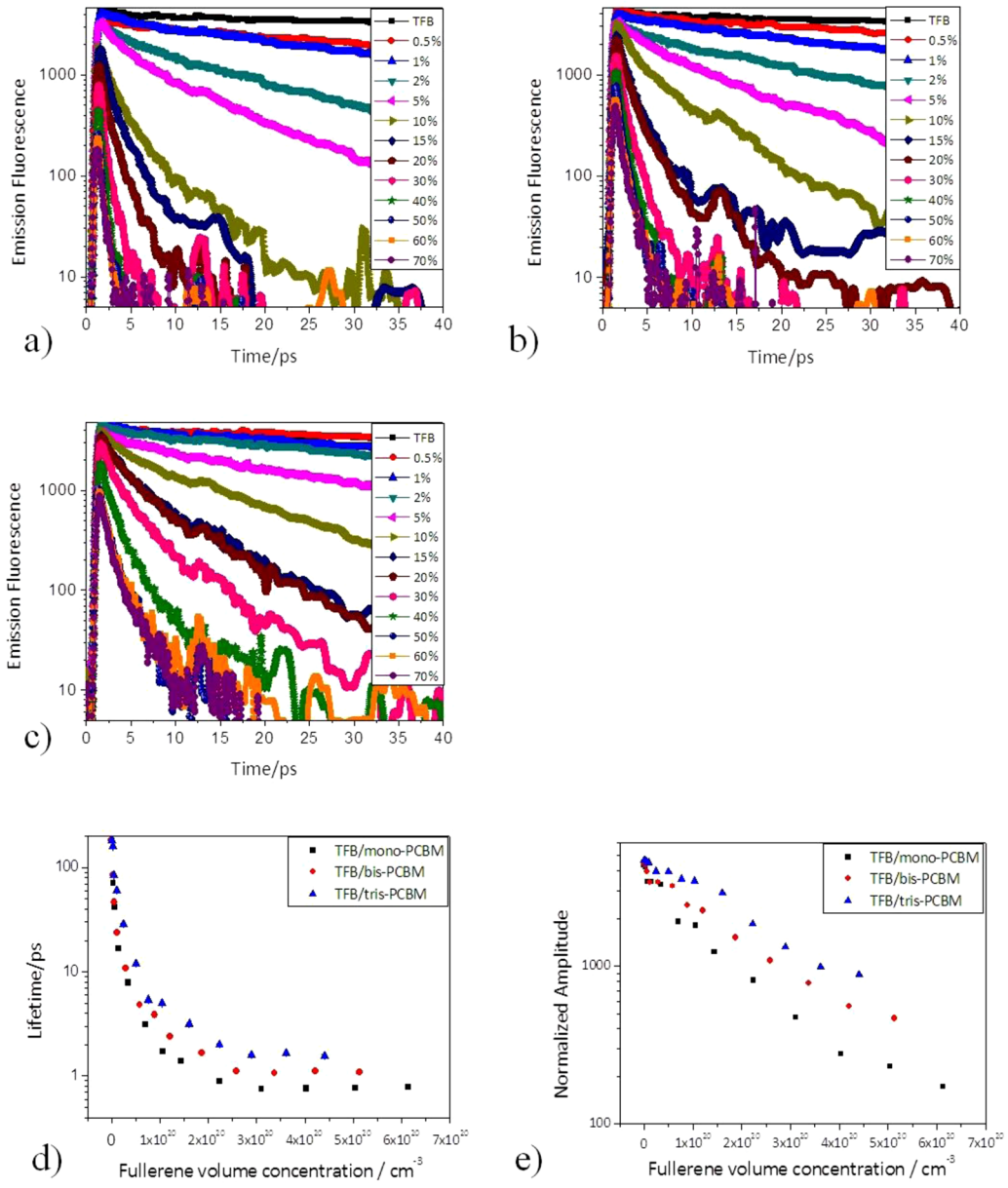

Figure 1. Time-resolved fluorescence decays of (a) TFB/mono-PCBM, (b) TFB/bis-PCBM, and (c) TFB/tris-PCBM. Excitation was at 400 nm, and the emission was detected at 460 nm. The intensity of the excitation beam is kept constant for all the measurements, and the data are corrected for the number of absorbed photons. Part (d) shows the decay times extracted from a single exponential fit of the data in (a)−(c). Part (e) shows the maximum fluorescence amplitude trend for the three compositions in (a)−(c). (Panels (d) and (e) are plotted against volume density of C_{60} units in the blend film).

harvesting limits charge generation.[9] Such studies can also determine the effect of blend morphology on exciton harvesting. Time-resolved PL measured on a subpicosecond to nanosecond time scale offers further information, such as the determination of exciton dynamics including excited state energy transfer processes and the mechanism of exciton PL quenching and dissociation at donor−acceptor interfaces. When performed on materials of carefully controlled composition or process history these measurements can yield information on the film microstructure and how it is affected by processing. Using suitable models it is possible then to evaluate the relative importance of energetic (ΔE) and structural (L_{ex}, domain size) factors in controlling exciton dissociation. For example, PL has been used as a probe of changes in microstructure due to annealing-induced phase segregation,[10] different acceptors,[11] or solvent-induced effects that may change the average size of the donor or acceptor domains.[12,13] Ultrafast PL has also been used to measure the effective exciton diffusion length in molecular materials by studying the dependence of the PL quenching on the thickness of an organic thin film on top of an acceptor layer.[14−16]Recently, there have also been studies of PL quenching as a function of fullerene concentration in polymer/fullerene blends.[17,18]

In this work we employ a femtosecond−picosecond time-resolved PL technique to evaluate the exciton diffusion length in amorphous, polyfluorene polymer films doped with different fullerene acceptors. We select an amorphous polymer to minimize processing-related variations in the morphology of the polymer phase and to have simpler, with respect to a crystalline polymer, exciton decay dynamics. The use of three

dx.doi.org/10.1021/jp404985q | J. Phys. Chem. C 2013, 117, 19832−19838

different acceptors with the same polymer increases confidence in the L_{ex} valueextracted by excluding acceptor-related effects and at the same time facilitates an investigation into the effect of the three acceptors' morphology on the quenching. In particular, we use PL quenching with transmission electron microscopy to relate differences in both quenching and exciton dissociation efficiency to blend film microstructure.

EXPERIMENTAL SECTION

Materials. The polymer [9,9-dioctylfluorene-co-*N*-(4-butylphenyl)-diphenylamine] (TFB) was used as the donor material, and three different types of fullerenes were used as acceptors: [6,6]-phenyl-C61 butyric acid methyl ester (most commonly called PCBM; for clarity in this work we will use mono-PCBM) and its multiadduct analogues bis-PCBM and tris-PCBM. Fullerene molecular structures are reported in Table S1 in the Supporting Information. The fullerene LUMO energies were found to be −3.71 eV (mono-PCBM), −3.56 eV (bis-PCBM), and −3.49 eV (tris-PCBM).[19]

Three sets of films varying acceptor concentrations from 0.5 to 70 wt % for the three acceptors were prepared. These samples were prepared from a 10 mg/mL TFB solution in chlorobenzene mixed appropriately with a 10 mg/mL mono-PCBM, bis-PCBM, or tris-PCBM chlorobenzene solution to obtain the desired blended concentration. The solution was spin coated in air onto Spectrosil quartz substrates at 1500 rpm for 45 s. The substrates had been precleaned by sonication in acetone and subsequently in isopropanol. All the preparation was done at room temperature. Absorption and emission spectra of all the prepared films were collected and are reported in Figure S1 in the Supporting Information.

For complementary diffusion length measurements, films of TFB polymer of thicknesses from 3.5 to 12 nm were spin coated onto glass substrates that had previously been coated with a 20 nm layer of TiO_2 by spray pyrolysis.

While TFB is not a practical OPV material because of its wide optical gap,[20] this polymer is of interest as a well-understood example of an amorphous polymer with microstructural properties similar to those of other, low gap, donor polymers. We select TFB for the current study partly because of its high photoluminescence quantum efficiency[21] and first-order transient PL decays that enable detailed analysis.

Time-Resolved Photoluminescence. The up-conversion experiments used the output from an ultrafast mode-locked Ti−sapphire oscillator (Newport Spectra-Physics Broadband MaiTai) with the wavelength fixed at 800 nm. The fundamental pulse duration was 70 fs at a repetition rate of 80 MHz. A portion of this fundamental beam was frequency-doubled to create the excitation beam with a wavelength of 400 nm. Both the gate and excitation beams were independently compressed using prism pair compressors. Photoluminescence from the sample was focused on a 200 μm BBO crystal and on the 800 nm gate beam. The generated sum frequency photons (corresponding to photoluminescence at 460 nm) were detected using a photomultiplier tube (R7207−01, Hamamatsu), and data were acquired using LabView software (Ultrafast Systems). The temporal resolution of the system was 150 fs. Sample degradation was avoided by performing the measurements under flowing nitrogen and using a translation stage to move the sample within the beam, removing the effect of photobleaching and providing data averaged across the whole of the sample. The photon density was kept well below 10^{15} cm^{-3} to perform the measurements below the exciton−exciton annihilation onset.

RESULTS AND DISCUSSION

Fluorescence decays for the three sets of samples are presented in Figure 1a−c, with the ratio of acceptor in the blend varied from 0.5 to 70 wt %. The signals have been corrected for the number of absorbed incident photons. As can be observed, the TFB fluorescence is efficiently quenched in all cases by the three acceptors, even with a very small weight percent of acceptors. The decays follow exponential kinetics, with the decay time decreasing with increasing fullerene concentration up to a saturation level that depends on the type of acceptor.

In this case, we cannot exclude that a small fraction of fullerene excitons will be excited at the same time as the TFB excitons. From the absorption coefficients of both TFB[20] and PCBM,[22] we estimate the PCBM exciton fraction to be less than 10% for blend films containing up to 70% fullerene by weight. Therefore, we do not expect exciton generation in the fullerene to significantly affect the conclusions.

The lifetimes obtained by fitting a single exponential to the data (starting at the maximum of the signal, thus excluding processes occurring within the response function) are reported in Figure 1d. Because it is important to account for the different molecular weights of the fullerene adducts, the data are plotted as a function of volume concentration of fullerene molecules, assuming a density of 1.0 g cm^{-3} for the polymer and for the fullerene side chains and a density for C_{60} cages of 1.5 g cm^{-3}. Lifetimes decrease rapidly as a function of fullerene loading up to $\sim 2 \times 10^{20}$ cm^{-3} (~30 wt % fullerene), at a similar rate for all three fullerenes. This trend is assigned to the shorter time taken for an exciton to find a fullerene quencher as fullerene concentration is increased. At higher concentrations, the lifetimes begin to saturate, but this occurs at different levels for all three acceptors. In particular, at higher acceptor concentration, TFB excitons in the tris-PCBM-based blends seem to live longer than those in the bis-PCBM blends, while the shortest lifetimes are seen in the PCBM blend films. This is also apparent from the kinetic traces in Figure 1a−c.

The trend of the peak fluorescence amplitude, corrected for the relative absorption, with acceptor concentration is reported in Figure 1e. For all three acceptors the amplitude decreases continuously with increasing fullerene loading. This amplitude signal decrease is assigned to the increasing probability that the exciton will reach an acceptor in a time shorter than the instrumental response (<150 fs) as more fullerene is added. For concentrations up to 1×10^{20} cm^{-3}, (approximately 20 wt % fullerene), the amplitude is comparable for all three fullerenes. At high fullerene loadings, the amplitude for PCBM reaches values that are lower than for those for the higher adducts, in agreement with the greater reduction in exciton lifetime reported above.

If the degree of quenching is interpreted as an indicator of the average distance from the photogenerated exciton to the nearest acceptor, then the saturation in quenching rate suggests that the concentration of fullerene finely dispersed with the polymer phase has saturated. This could occur if the fullerene reaches its miscibility limit. The presence of the saturation has not been reported in previous studies where slower time resolution was used and smaller acceptor loading was investigated.[17] Previous studies have shown that blends of amorphous polymer with PCBM typically show a two-phase

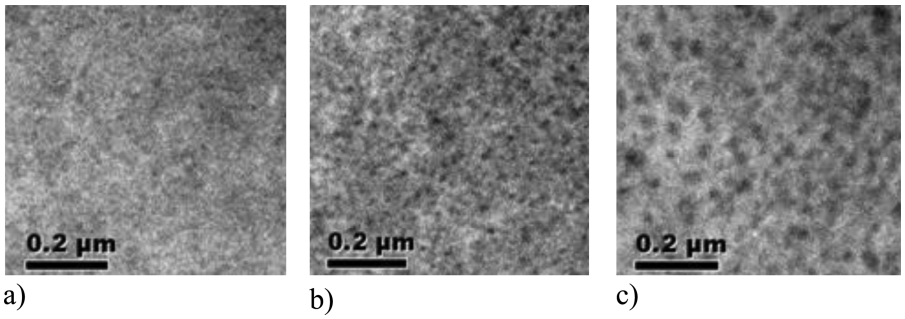

Figure 2. TEM images for 50% blends: (a) TFB/mono-PCBM, (b) TFB/bis-PCBM, (c) TFB/tris-PCBM.

structure, consisting of a mixed polymer/fullerene phase and a separated phase of fullerene aggregates.[23,24]

Differences in saturation level between fullerenes could result from two different factors: either different degrees of mixing of the fullerenes into the polymer phase or a different probability of exciton dissociation once the interface is reached. Both explanations are plausible given that additional side chains are, first, likely to influence the interaction energy between polymer and fullerene and hence the miscibility of the fullerene in the polymer matrix,[25] and second, are capable of slowing down the average rate of intermolecular charge transfer between polymer and fullerene. In other words, upon increasing the number of fullerene side chains, the miscibility limits for the blends with similar weight concentrations can be different, producing a diverse mixing between the polymer and the acceptor; the local environment that the polymer exciton sees, in the presence of the three acceptors, is different. In particular, fluorescence decays of TFB/mono-PCBM, bis-PCBM, and tris-PCBM blend films present different saturation levels, and the saturation appears at a different concentration for each acceptor. This corresponds to the condition of a different aggregation starting limits for mono-PCBM, bis-PCBM, and tris- PCBM.

To explore the effect of side-chains on blend film microstructure, we have taken TEM images of 50 wt % fullerene blended TFB films (Figure 2). The images in Figure 2a–c show a heterogeneous structure, indicating that the fullerene has phase-segregated morphology from the polymer in each case. The images suggest a finer mixing for the blends with mono-PCBM compared to those with bis-PCBM, while significantly larger domains are evident for the blends with tris-PCBM. Similar behavior has been observed for blends of the same three fullerenes with poly-3-hexylthiophene (P3HT)[25] and is supported by differential scanning calorimetric measurements of those blends.[11] The microscopic data are consistent with different miscibility limits for the different blends, however, they are also consistent with similar miscibility and different fullerene domain sizes due to different fullerene–fullerene interactions.

Regarding the possibility that different miltiadducts lead to different quenching efficiencies in the blends, presious studies have presented diversified data. In the case of fullerene multiadducts with regioregular (P3HT)/fullerene blend films, some dependence of PL quenching on fullerene yield has been observed,[11] although no dependence of charge yield on fullerene type has been observed.[25] Previous studies on similar polyfluorene/fullerene blends showed that multiadduct types can influence the rate of photoinduced charge transfer because triplet formation is more likely for PFB/tris-PCBM than for TFB/mono-PCBM, despite the same nominal driving energy.[24] A reduced average rate of charge transfer from a given polymer to a higher fullerene adduct, at the same driving energy, could be expected as a result of both poorer electric coupling and higher energetic disorder.[19,26]

Model. In order to evaluate the different explanations for the concentration dependence of the fluorescence kinetics, we use a simple model of exciton dynamics. We consider that excitons are removed either by natural singlet decay, at rate k_R, or by diffusion of the exciton into a space containing a fullerene. Then the volume density of excitons will vary according to the following equations:

$$\frac{dx}{dt} = -k_R x - k_Q x$$

where

$$k_Q = \frac{6P_Q p_A D a_{ex}}{{a_A}^3}. \quad (1)$$

Here we have expressed k_Q as the product of the rate at which the exciton diffuses its own length ($(6D)/({a_{ex}}^3)$, with a_{ex} length step of the random walk) with the probability that the new volume contains an acceptor ($(n{a_{ex}}^3)/({a_A}^3)$) where a_A is the diameter of the fullerene, and the probability that the exciton dissociation occurs, $P_Q k_Q$ can then be expressed in terms of k_R using the definition of exciton diffusion length ($D = {L_{ex}}^2/t_R = k_R {L_{ex}}^2$). Thus

$$k_Q = \frac{6P_Q n {L_{ex}}^2 a_{ex}}{{a_A}^3 k_R} \quad (2)$$

A useful quantity is the enhancement of the net exciton decay rate relative to the polymer alone, i.e.,

$$\Gamma = \frac{k_R + k_Q}{k_R} = \frac{6P_Q n {L_{ex}}^2 a_{ex}}{{a_A}^3} + 1 \quad (3)$$

In the limit where the concentration n of the acceptor in the polymer phase saturates at a value, n_{MAX}, the rate enhancement then plateaus at the value

$$\Gamma = \frac{K}{k_R} = \left(\frac{6P_Q {L_{ex}}^2 a_{ex}}{{a_A}^3}\right) n_{MAX} + 1 \quad (4)$$

The only parameters that should vary between acceptors are the dissociation probability P_Q and the miscibility limit, n_{MAX}. Let us consider each case in turn. If P_Q varies, then Γ will be scaled by the factor P_Q. If n_{MAX} varies, then all Γ values should follow the same form before saturation and differ only in the saturation levels. Figure 3 shows the experimental rate enhancement data calculated from the data in Figure 1d.

dx.doi.org/10.1021/jp404985q | J. Phys. Chem. C 2013, 117, 19832–19838

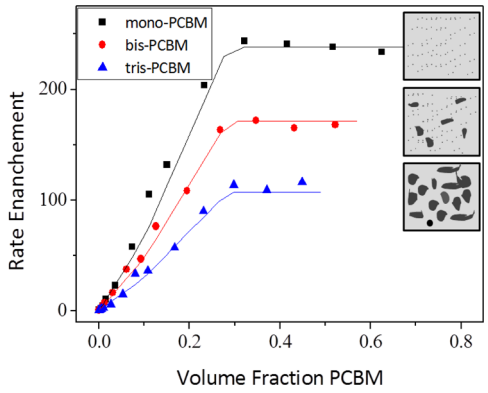

Figure 3. Rate enhancement at each concentration of fullerene from the experimental data (black diamonds, TFB/mono-PCBM; red circles, TFB/bis-PCBM; blue triangles, TFB/tris-PCBM) and the modeled curves (black line, TFB/mono-PCBM; red line, TFB/bis-PCBM; blue line, TFB/tris-PCBM). Bis-PCBM and tris-PCBM are fitted with a quenching efficiency of 0.7 and 0.5 respectively.

Note that the data for different fullerenes show different gradient of Γ with n and different plateau values but show saturation at similar fullerene volume concentrations. This suggests that the data are more easily explained by a variation in P_Q. We then fit the data for the PCBM blend to eqs 3 and 4, assuming that the fullerene is randomly dispersed and that the quenching probability is maximum ($P_Q = 1$). Both assumptions are reasonable given that PCBM is the most easily dispersed fullerene and has the largest driving force for exciton quenching. This fitting allows us to determine $L_{ex}^2 a_{ex}$ to be 124 nm[3]. This procedure yields a range of values for L_{ex} from 8 nm (a_{ex} = 2 nm) to L_{ex} = 11 nm (a_{ex} = 1 nm). Keeping these values of L_{ex} and a_{ex}, we then proceed to fit the experimental data for the other two blends by varying P_Q.

The data are well fitted by reproduced P_Q values of $P_Q = 0.75$ for bis-PCBM and $P_Q = 0.5$ for tris-PCBM. The reduced quenching efficiency appears to explain the variations in both gradient and plateau level of Γ, and fit the transition to saturation well.

Thus the data appear to be explained by a fullerene adduct-dependent exciton dissociation efficiency together with an adduct-dependent miscibility limit for the fullerene in the polymer, which is schematically represented in Figure 3. However, it is possible that the different gradients could also be affected by differences in fullerene nucleation and growth rates. Further microstructural details would be needed to assess this.

A reduced quenching probability for higher PCBM adducts indicates a reduced rate of electron transfer from photoexcited polymer to fullerene when the adduct number increases. This could result from several factors. The rate of electron transfer is controlled by the electronic coupling and the driving energy. Higher adduct number reduces both coupling through the insulating affect of additional nonconjugated side chains and driving energy through the strain-induced raising of the fullerene LUMO energy. In the present case, the variations in driving energy are unlikely to explain the observed fullerene dependence of exciton dissociation because the driving energy is large in all cases (polymer singlet−CT complex energy >1 eV), and other cases are known in which much lower driving energies still result in efficient electron transfer. We tentatively suggest that the reduced dissociation rate is due to the poor electronic coupling between higher adducts and the polymer backbone, partly caused by the large polymer side chains.

This fluorescence decays-based method of measuring polymer exciton diffusion has numerous advantages compared to other optical techniques used to measure the diffusion length in polymers, as has been discussed before.[17] In contrast to other methods, in the present case the measured exciton diffusion length corresponds to the spatial diffusion length, which is more realistic (i.e., the same sample preparation is performed under the same conditions as the real solar cell devices) with respect to the two-dimensional length obtained from surface quenching measurements[27,28] or in an oxygen environment.[29] When the measurements are performed using pumping energies that are considered to be below the exciton−exciton annihilation limit, the problem of artifact shortening in the fluorescence decays is also avoided. The simplicity of sample preparation and experimental methods makes this methodology very useful for evaluating the exciton diffusion length in various polymers using the same acceptor[17] or for comparing the effect of the morphology using similar acceptors with the same polymer, as we presented in this work. Indeed, it has been shown that for various blend compositions both diffusion length and information about the thin film microstructure of the blends can be obtained when different acceptors are used.

To ascertain an independent and indeed separate estimation of the diffusion length we performed a surface quenching experiment using TiO_2 as the quencher. Dilute solutions (see Supporting Information) of TFB were spin-cast onto a 20 nm thick TiO_2 substrate in order to produce very thin layers of TFB. The thickness of each film was determined by absorption measurements (knowing the absorption coefficient of TFB[20] and from our independent measurements on films of known thickness). In Figure 4, the integral of the fluorescence emission

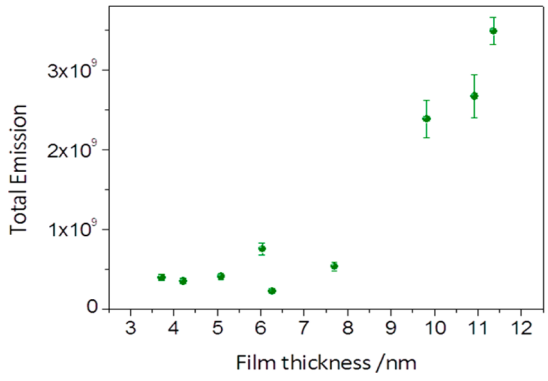

Figure 4. Total emitted fluorescence (after excitation at 400 nm) for TFB samples of different thicknesses on a TiO_2 substrate that is 20 nm thick.

for the different samples is reported as a function of the film thickness. A jump in the value of the total emitted fluorescence is clearly observed between thicknesses of 8 and 10 nm, indicating the critical value for diffusion length for the TFB polymer exciton lies in this size interval. This value for L_{ex} is in a good agreement with that evaluated by our model of the ultrafast decay data.

CONCLUSIONS

In this study we employed femtosecond−picosecond time-resolved fluorescence to study emission quenching in a series of

dx.doi.org/10.1021/jp404985q | J. Phys. Chem. C 2013, 117, 19832−19838

polymer/fullerene blends. Concentration-dependent data for three fullerene-based acceptors have allowed the direct determination of the exciton diffusion length in bulk heterojunction blends. The good agreement with an independent experimental technique has also been reported. Concentration dependence of ultrafast fluorescence decays together with the dependence of steady state PL quenching on polymer film thickness fixes the exciton diffusion length in the TFB polymer to ∼9 nm. Weaker PL quenching observed in blend films made with fullerene multiadducts can be explained by a combination of two factors: fullerene aggregation and lower quenching efficiency. Further studies will be needed to distinguish quantitatively the influences of quenching efficiencies and miscibility limits for the different fullerenes studied.

Higher aggregation morphology in blend films with multiadducts, especially with tris-PCBM, is supported by TEM images. Time-resolved PL data for blends with a range of fullerenes is a good way to determine exciton diffusion lengths and also to identify the effects of fullerene aggregation and morphology, provided that the quenching efficiency can be independently estimated.

■ ASSOCIATED CONTENT

Supporting Information

Full experimental details on materials, spectroscopic data, techniques, and mathematical model. This material is available free of charge via the Internet at http://pubs.acs.org.

■ AUTHOR INFORMATION

Corresponding Authors

*s.a.haque@imperial.ac.uk.
*jenny.nelson@imperial.ac.uk.

Notes

The authors declare no competing financial interest.

■ ACKNOWLEDGMENTS

The authors acknowledge funding from the Royal Society, the Grantham Institute for Climate Change, and EPSRC via the Grand Challenge (EP/F056389/1), Excitonic Supergen (EP/G031088/1), and UK-India (EP/H040218/1) programmes. S. A. Haque acknowledges the Royal Society for a Royal Society University Research Fellowship. The TFB polymer used in these experiments was synthesised by the Sumitomo Chemical Company, and we thank Donal Bradley for access to this material.

■ REFERENCES

(1) Green, M. A.; Emery, K.; Hishikawa, Y.; Warta, W. For the Solar Cell Efficiency Tables (version 39). *Prog. Photovoltaics* **2012**, *20*, 12−20.

(2) Service, R. F. Outlook Brightens For Plastic Solar Cells. *Science* **2011**, *332*, 293−293.

(3) Veldman, D.; Ipek, O.; Meskers, S. C. J.; Sweelssen, J.; Koetse, M. M.; Veenstra, S. C.; Kroon, J. M.; van Bavel, S. S.; Loos, J.; Janssen, R. A. J. Compositional and Electric Field Dependence of the Dissociation of Charge Transfer Excitons in Alternating Polyfluorene Copolymer/Fullerene Blends. *J. Am. Chem. Soc.* **2008**, *130*, 7721−7735.

(4) Frost, J. M.; Cheynis, F.; Tuladhar, S. M.; Nelson, J. Influence of Polymer-Blend Morphology on Charge Transport and Photocurrent Generation in Donor−Acceptor Polymer Blends. *Nano Lett.* **2006**, *6*, 1674−1681.

(5) Benson-Smith, J. J.; Ohkita, H.; Cook, S.; Durrant, J. R.; Bradley, D. D. C; Nelson, J. Charge Separation and Fullerene Triplet Formation in Blend Films of Polyfluorene Polymers with [6,6]-Phenyl C61 Butyric Acid Methyl Ester. *Dalton Trans.* **2009**, *45*, 10000−10005.

(6) Hallermann, M.; Haneder, S.; Da Como, E. Charge-Transfer States in Conjugated Polymer/Fullerene Blends: Below-Gap Weakly Bound Excitons for Polymer Photovoltaics. *Appl. Phys. Lett.* **2008**, *93*, 53307−53311.

(7) Loi, M. A.; Toffanin, S.; Muccini, M.; Forster, M.; Scherf, U.; Scharber, M. Charge Transfer Excitons in Bulk Heterojunctions of a Polyfluorene Copolymer and a Fullerene Derivative. *Adv. Funct. Mater.* **2007**, *17*, 2111−2116.

(8) Peumans, P.; Forrest, S. R. Separation of Geminate Charge-Pairs at Donor−Acceptor Interfaces in Disordered Solids. *Chem. Phys. Lett.* **2004**, *398*, 27−31.

(9) Piris, J.; Dykstra, T. E.; Bakulin, A. A.; van Loosdrecht, P. H. M; Knulst, W.; Trinh, M. T.; Schins, J. M.; Siebbeles, L. D. A. Photogeneration and Ultrafast Dynamics of Excitons and Charges in P3HT/PCBM Blends. *J. Phys. Chemistry C* **2009**, *113*, 14500−14506.

(10) Keivanidis, P. E.; Clarke, T. M.; Lilliu, S.; Agostinelli, T.; Macdonald, J. E.; Durrant, J. R.; Bradley, D. D. C.; Nelson, J. Dependence of Charge Separation Efficiency on Film Microstructure in Poly(3-hexylthiophene-2,5-diyl):[6,6]-Phenyl-C61 Butyric Acid Methyl Ester Blend Films. *Phys. Chem. Lett.* **2010**, *1*, 734−738.

(11) Guilbert, A. Y.; Reynolds, L. X.; Bruno, A.; Pires, E.; Macdonald, J. E.; Stingelin-Stutzmann, N.; Haque, S. A.; Nelson, J. Effect of Multiple Adduct Fullerenes on Microstructure and Phase Behavior of P3HT:Fullerene Blend Films for Organic Solar Cells. *ACS Nano* **2012**, *6*, 3868−3875.

(12) Hoppe, H.; Sariciftci, N. S. Morphology of Polymer/Fullerene Bulk Heterojunction Solar Cells. *J. Mater. Chem.* **2006**, *16*, 45−6.

(13) Morvillo, P.; Grimaldi, I. A.; Diana, R.; Loffredo, F.; Villani, F. Study of the Microstructure of Inkjet-Printed P3HT:PCBM Blend for Photovoltaic Applications. *J. Mater. Sci.* **2013**, *48*, 2920−2927.

(14) Scully, R.; McGehee, M. D. Effects of Optical Interference and Energy Transfer on Exciton Diffusion Length Measurements in Organic Semiconductors. *J. Appl. Phys.* **2006**, *100*, 34907−34912.

(15) Shaw, P. E.; Ruseckas, A.; Samuel, I. D. W. Exciton Diffusion Measurements in Poly(3-hexylthiophene). *Adv. Funct. Mater.* **2008**, *20*, 3516−3520.

(16) Kroeze, J. E.; Savenije, T. J.; Vermeulen, M. J. W.; Warman, J. M. Contactless Determination of the Photoconductivity Action Spectrum, Exciton Diffusion Length and Charge Separation Efficiency in Polythiophene-Sensitized TiO_2 Bilayers. *J. Phys. Chem. B* **2003**, *107*, 7696−7705.

(17) Mikhenko, O. V.; Azimi, H.; Scharber, M.; Morana, M.; Blom, P. W. M.; Loi, M. A. Exciton Diffusion Length in Narrow Bandgap Polymers. *Energy Environ. Sci.* **2012**, *5*, 6960−6965.

(18) Ward, A. J.; Ruseckas, A.; Samuel, I. D. W. A Shift from Diffusion Assisted to Energy Transfer Controlled Fluorescence Quenching in Polymer−Fullerene Photovoltaic Blends. *J. Phys. Chem. C* **2012**, *116*, 23931−23937.

(19) Frost, J. M.; Faist, M. A.; Nelson, J. Energetic Disorder in Higher Fullerene Adducts: A Quantum Chemical and Voltammetric Study. *Adv. Mater.* **2010**, *22*, 4881−4884.

(20) Ramsdale, C. M.; Greenham, N. C. The Optical Constants Of Emitter And Electrode Materials in Polymer Light-Emitting Diodes. *J. Phys. D: Appl. Phys.* **2003**, *36*, 29.

(21) Redecker, M.; Bradley, D. D. C.; Inbasekaran, M.; Wu, W. W.; Woo, E. P. High Mobility Hole Transport Fluorene-Triarylamine Copolymers. *Adv. Mater.* **1999**, *11*, 241−246.

(22) Hoppe, H.; Sariciftci, N. S.; Meissner, D. Optical Constants of Conjugated Polymer/Fullerene Based Bulk-Heterojunction Organic Solar Cells. *Mol. Cryst. Liq. Cryst.* **2002**, *385*, 233−239.

(23) Dyer-Smith, C.; Reynolds, L. X.; Bruno, A.; Bradley, D. D. C.; Haque, S. A; Nelson, J. Charge Separated State Energies and Fullerene Triplet Formation in Fullerene Multi-Adduct Blends for Organic Solar Cells. *Adv. Funct. Mat.* **2010**, *20*, 2310−2316.

(24) Van Duren, J. K. J.; Yang, X.; Loos, J.; Bulle-Lieuwma, C. W. T.; Sieval, A. B.; Hummelen, J. C.; Janssen, R. A. J. Relating the

Morphology of Poly(*p*-phenylene vinylene)/Methanofullerene Blends to Solar-Cell Performance. *Adv. Funct. Mater.* **2004**, *14*, 425−434.
(25) Faist, M. A.; Keivanidis, P. E.; Foster, S.; Wöbkenberg, P. H.; Anthopoulos, T. D.; Bradley, D. D. C.; Durrant, J.; Nelson, J. Effect of Multiple Adduct Fullerenes On Charge Generation and Transport in Photovoltaic Blends with Poly(3-Hexylthiophene-2,5-Diyl). *J Poly. Sci. B: Polymer Physics* **2011**, *49*, 1−11.
(26) Peumans, P.; Uchida, S.; Forrest, S. R. Efficient Bulk Heterojunction Photovoltaic Cells Using Small-Molecular-Weight Organic Thin Films. *Nature* **2003**, *425*, 158−162.
(27) Westenhoff, S.; Howard, I. A.; Friend, R. H. Probing the Morphology and Energy Landscape of Blends of Conjugated Polymers with Sub-10 nm Resolution. *Phys. Rev. Lett.* **2008**, *101*, 016102−0161106.
(28) Westenhoff, S.; Ian, A. H.; Hodgkiss, J. M.; Kirov, K. R.; Bronstein, H. A.; Williams, C. K.; Greenham, N. C.; Friend, R. H. Charge Recombination in Organic Photovoltaic Devices with High Open-Circuit Voltages. *J. Am. Chem. Soc.* **2008**, *130*, 13653−13659.
(29) Luer, L.; Egelhaaf, H. J.; Oelkrug, D.; Cerullo, G.; Lanzani, G.; Huisman, B. H.; de Leeuw, D. Oxygen-Induced Quenching of Photoexcited States in Polythiophene Films. *Org. Electron.* **2004**, *5*, 83−89.